Niche Partitioning in the Rimicaris Exoculata Holobiont: The Case of the First Symbiotic Zetaproteobacteria

Marie-Anne Cambon-Bonavita
Ifremer
Johanne Aubé
Ifremer
Valérie Cueff-Gauchard
Ifremer
Julie Reveillaud (reveillaud.j@gmail.com)
INRA Centre de Montpellier https://orcid.org/0000-0002-2185-6583

Research

Keywords: Niche partitioning, Rimicaris, Metagenome-Assembled Genomes, Zetaproteobacteria, holobiont, hydrothermal vents

Posted Date: June 4th, 2020

DOI: https://doi.org/10.21203/rs.3.rs-33129/v1

Version of Record: A version of this preprint was published at Microbiome on April 12th, 2021. See the published version at https://doi.org/10.1186/s40168-021-01045-6.

Abstract

Background

Mutualistic symbioses between invertebrate animals and chemosynthetic bacteria are at the basis of Life in hydrothermal vent ecosystems. The shrimp *Rimicaris exoculata*, which dominates animal fauna along the Mid Atlantic Ridge, houses in its cephalothorax a complex bacterial community including *Campylobacteria*, *Gamma- Delta-* and some recently discovered iron oxyhydroxides-coated *Zetaproteobacteria*. This epibiotic consortium uses iron, sulfide, methane and hydrogen as energy sources. Here, we used a DNA extraction procedure adapted to recalcitrant embedded bacteria and generated shotgun metagenomes from *Rimicaris exoculata* cephalothoracic epibiotic community. We aimed reconstructing symbiotic genomes from specimen collected in three geochemically contrasted vent fields, TAG, Rainbow and Snake Pit to unravel the specificity, variability and adaptation of host-microbes associations.

Results

Using these data we were able to reconstruct 49 high quality metagenome-assembled genomes (MAGs) from TAG and Rainbow vents fields. Most critically, two MAGs in our collection were affiliated to *Zetaproteobacteria* and had no close relatives (ANI < 77% from the closest relative *Ghiorsea bivora* isolated from TAG and <88% between each other), suggesting potential novel species. Genes for CBB carbon fixation, iron and sulfur oxidation, as well as nitrate reduction, occurred in both MAGs. However, genes for hydrogen oxidation and quorum sensing as well as multicopper oxidases occurred in one MAG only, suggesting shared and specific potential functions for these two novel *Zetaproteobacteria* symbiotic lineages. Overall, we observed highly similar symbionts that co-exist in a single shrimp at both basaltic TAG and ultramafic Rainbow vent sites. Nevertheless, further insights into the seemingly functional redundancy between those epibionts revealed important differences.

Conclusion

These data highlight microniche partitioning in the *Rimicaris* holobiont and confirm recent works that show functional diversity enables multiple symbiont strains to coexist in animals from hydrothermal vents.

Background

Life in deep-sea hydrothermal vent ecosystems is based on chemosynthetic primary production, mainly sustained by symbiotic associations with chemosynthetic bacteria (Dubilier 2008). The shrimp *Rimicaris exoculata* dominates the fauna of hydrothermal sites along the Mid Atlantic Ridge [1, 2]. The species lives in dense aggregates at a warm part of the hydrothermal environment, 3–25 °C [3]. Adults harbor a complex bacterial community, one located in their hypertrophied cephalothoracic cavity and a second in the digestive system where long microbial filaments are identified but their role is still enigmatic [4–6].

The cephalothoracic cavity microbiote was first described as a single sulfoxidizing filamentous epsilonproteobacterial lineage [7]-(*Epsilonproteobacteria* being renamed *Campylobacteria*, [8, 9]. It nevertheless proved to be much more diverse including *Alpha* and *Gammaproteobacteria*- [10–13], *Deltaproteobacteria* [10, 14, 15] and more recently discovered, *Zetaproteobacteria* [16]. *In vivo* experiments provide evidence for direct nutritional transfers from bacteria to the host directly across the cephalothoracic chamber integument and therefore indicate a true mutualistic trophic association [17]. In addition, *in silico* analyses show four potential metabolic pathways (iron, sulfide, methane and hydrogen oxidation) may co-occur within this community [10, 16]. This diversity of metabolisms suggests the epibiotic community associated with *R. exoculata* is highly plastic, providing a potential adaptive advantage for the shrimp thriving in highly dynamic hydrothermal mixing zones that could explain the clear success of the holobiont (i.e., the animal in interaction with its symbiotic counterparts) in colonizing geochemically contrasted hydrothermal vents all along the Mid-Atlantic Ridge. However, although previous metagenomic work identified diverse microbial populations, authors focused on dominant metabolisms and community members. Briefly, Jan and colleagues [16] focused on carbon fixation pathways (rTCA and CBB cycles for *Campylobacteria* and *Gamma/ Zetaproteobacteria* respectively), sulfur, hydrogen and nitrogen cycles, stress response and interaction with host. They identified taxobins as submetagenomes but did not undergo genome reconstruction. Recently, Jian et al. [15] focused on *Deltaproteobacteria* and described an abundant and novel Candidatus *Desulfobulbus rimicarensis* species with specific symbiotic traits. However, the functional capacities and evolutionary relationships of the remaining epibionts, and notably the *Zetaproteobacteria* in comparison to their free-living counterparts still remain unknown.

The iron-oxidizing *Zetaproteobacteria Mariprofundus ferrooxydans* PV-1 and JV-1 isolates were first described from the Loihi hydrothermal systems in Hawaii [18, 19]. *Zetaproteobacteria* have since then been described from very distinct habitats showing high ferrous iron concentrations including coastal sediments, steel corrosion biofilms, saline terrestrial springs [20, 21]. They are also reported at the studied TAG, Rainbow and Snake Pit hydrothermal sites where they dominate iron rich mat microbial communities [22]. These specialized yet diverse bacteria are well adapted to microaerobic growth on Fe(II) and play an important role in the biogeochemical iron cycle within these diverse ecosystems, where abiotic iron oxidation was first supposed to be the rule [23, 24]. *Zetaproteobacteria* have been described and cultivated as strict microaerophilic chemoautotrophic bacteria [19, 25], but genomic data suggest possible mixotrophy [24, 26]. Some free-living Fe(II)-oxidizing *Zetaproteobacteria* cells form sheaths or stalks, controlling Fe mineral growth near the surface of the cell [21]. Biotic iron oxidation reactions are well documented in the *Rimicaris* cephalothoracic cavity through observations of iron oxyhydroxide particles embedding microbial cells, giving them a rusty color at the end of their moult cycle [27, 28]. Since, it is possible these coating with iron oxyhydroxides tightly attached to iron substrates [27, 28] increase the difficulty to extract genomic DNA from these epibionts. The functional characteristics of the supposedly first reported host-associated *Zetaproteobacteria* therefore remain undetermined due to low DNA recovery [16].

Apart from these, reconstructing and separating highly similar genomes from metagenomes, notably from complex host-associated microbial communities, remained until recently, a challenge. The presence of closely related strains can increase assembly breaks, resulting in short orphan contigs that cannot be grouped together nor further analyzed. In addition, unlike for symbionts that are constrained in a specific organ such as tubeworm trophosomes [29], and despite precautious DNA extraction protocols, host contamination is unavoidable and can end up in a high number of host-associated contiguous sequences. Therefore, efforts to understand the epibiont community functioning are in its infancy. In particular, it remains unknown whether the highly diverse *Rimicaris* epibiont community is composed of specialists adapted to microniches that possibly complement or interact with each other through syntrophy, or rather of generalists able to perform a wide range of functions depending on the environmental conditions.

Here, we used a directed DNA extraction procedure adapted to maximize iron-embedded bacteria DNA recovery (including *Zetaproteobacteria)* followed by shotgun metagenomics and advanced binning strategies to reconstruct novel *Rimicaris exoculata* symbiotic genomes. We collected specimen from three geochemically contrasted hydrothermal vent along the MAR, and attempted to unravel their microbial metabolic potential. Snake Pit and TAG are two basaltic hydrothermal based systems located at 3460 m depth and Rainbow, an ultramafic-hosted hydrothermal vents is located at 2400 m depth. Briefly, basaltic-hosted sites have fluids mainly enriched in sulfur and minerals while ultramaphic ones present fluids relatively depleted in sulfur but enriched in methane, hydrogen and ferrous iron [30]. We here investigated functional diversity and assess potential niche differentiation at the level of genomes within and between sites in order to decipher the functioning of the *Rimicaris* epibiont community as a whole and to better understand animal-epibiont interactions at fine genomic scale.

Methods

Sample collection

We collected *Rimicaris exoculata* specimens using a suction sampler manipulated by the Remote Operated Vehicle (ROV) Victor 6000 on board on the research vessel *Pourquoi pas?*. Samples were taken from three hydrothermal sites on the Mid Atlantic Ridge (Fig. 1): Rainbow (36°13.760' N − 33°54.170' W, 2292 m depth) during the MoMAR (Leg2, August 25 to September 15, 2008, https://doi.org/10.17600/8010140) and the Biobaz cruise (August 02 to 21, 2013, http://dx.doi.org/10.17600/13030030), TAG (26° 8.237' N − 44° 49.563' W, 3625 m depth) and Snake Pit (23°22.140' N − 44°57.054' W, 3495 m depth) during the BICOSE cruise (January 11 – February 10 2014, http://dx.doi.org/10.17600/14000100), respectively. We rapidly froze Biobaz and BICOSE samples at -80 °C on board for downstream genomic DNA extraction. We dissected branchiostegite and scaphognatite of MoMAR specimen directly onboard under sterile conditions, fixed them for three hours in 3% formaldehyde seawater solution and stored them frozen in PBS/Ethanol 1:1 until further use for FISH experiments.

DNA extraction and estimation of Zetaproteobacteria proportion using qPCR

We performed sterile dissections in the lab on thawed samples before total genomic DNA extraction of the six *Rimicaris* cephalothoracic appendages (2 branchiostegites + 2 scaphognathites + 2 exopodites). We used the DNA extraction kit Nucleospin Soil (Macherey-Nagel) following manufacturer's instructions, and a preliminary vortex step of 5 min. As noted, *Zetaproteobacteria* have been previously found embedded in iron particles, which impair DNA extraction. To maximize DNA recovery, we aseptically crushed each sample in a mortar in iced lysis buffer before extraction. Then, we verified *Zetaproteobacteria* DNA presence and relative abundance in our *Rimicaris* DNA extracted samples. We amplified the 16S rRNA encoding gene of *Zetaproteobacteria* and bacteria using specific 672F (5'-CGGAATTCCGTGTGTAGCAGT-3') and 837R (5'-GCCACWGYAGGGGTCGATACC-3') *Mariprofundus ferrooxydans* primers [31] and universal primers 1369F (5'-CGGTGAATACGTTCYCGG-3') and 1492R (5'-GGWTACCTTGTTACGACTT-3') [32] respectively. We performed qPCR reactions in a final volume of 25 µl using PerfeCTa SYBR Green SuperMix ROX on a StepOnePlus™ Real-Time PCR System (Applied Biosystems), 1 ng of DNA template and 900 nM primers. 41 cycles were performed including one hot-start polymerase activation cycle (95 °C, 10 min) and 40 cycles of denaturation (95 °C, 15 s) followed by a hybridization and elongation step (60 °C, 60 s). We obtained standard curves from 10-fold serial dilutions (20-2.10^8 copies per microliter) of plasmids containing 16S rRNA genes of *Mariprofundus ferroxidans* DSM23021 and *Vibrio diabolicus* HE800, respectively. Each reaction was run in triplicates. We assessed the quality of qPCR runs based on melting curves and measured efficiencies; the R of standard curves generated by qPCR and efficiency of the reaction were above 0.998 and 90%, respectively. We checked those estimates were roughly equivalent for both *Zetaproteobacteria* and total bacteria. qPCR results were expressed in copy number per DNA ng. The *Zetaproteobacteria* 16S rRNA results were expressed as percent of bacteria 16S rDNA.

Microbial community DNA preparation and sequencing

We analyzed six *Rimicaris* individuals (hereafter referred to as RE5, RE6 from TAG site; RE12, RE13, from Rainbow site and RE3, RE7 from Snake Pit) for shotgun sequencing of total community DNA. We quantified DNA using the Nanodrop 1000. We sheared DNA to 175 bp using a Covaris S-series sonicator and completed metagenomic library construction using the Ovation Ultralow Library DR multiplex system (Nugen) following manufacturer's instructions. We performed metagenomic sequencing on an Illumina HiSeq 1000 and a NextSeq at the W.M. Keck sequencing facility at the Marine Biological Laboratory. All libraries were paired-end, with a 30 bp overlap, resulting in an average merged read length of 170 bp.

Metagenomic analysis

We trimmed adaptors using bbduk from bbmap 38.22 [33] after which we processed reads using a snakemake [34] workflow implemented in anvi'o v5 (http://merenlab.org/2018/07/09/anvio-snakemake-workflows/) [35]. Briefly, we relied upon illumina-utils v1.4 [36] with the 'iu-filter-quality-minoche' program with default parameters for sequence quality filtering.

We co-assembled two metagenomic datasets per site using Megahit 1.1.3 [37] and the –metasensitive mode, discarding contigs smaller than 1000 bp. We generated an anvi'o contigs database from assembled contigs for each of the three co-assemblies, using the anvi-gen-contigs-database program that uses Prodigal v2.6.3 [38] to identify ORFs and compute tetranucleotide frequency values in each contig. We realized an HMM profiling on resulting contigs databases using the program 'anvi-run-hmms' and assigned gene functions using the program 'anvi-run-ncbi-cogs' as well as KEGG function with kofamscan [39]. We then used FeGenie to identify canonical iron genes [40].We assigned taxonomy determined by the Genome Taxonomy Database (GTDB) using the anvi-run-scg-taxonomy program. We performed read recruitment analyses with Bowtie v2.3.4 [41]. Briefly, we profiled the short reads from each of the six individual metagenomes recruited onto the contigs from the three co-assemblies using the program 'anvi-profile'. We used the option "all-against-all' to map reads from each individual sample onto each of the 3 co-assemblies. We then merged resulting anvi'o profile databases for each sample using the program 'anvi-merge'. We realized an automatic binning using CONCOCT v1.1.0 through the program 'anvi-cluster-with-concoct (using half of the estimated genome number found with the single-copy core genes) followed by manual refinement for each co-assembly. Since our study was based on single assemblies for each site, rather than on a co-assembly of all data together, we afforded a dereplication of metagenome-assembled genomes (MAGs) from the different studied sites with the aim to remove very closely related genomes and avoid multiple high quality alignment during subsequent sequencing reads mapping steps. We dereplicated MAGs with drep v 2.3.2 using a coverage threshold ranging from 0.10 to 0.75 for comparison and an ANI > 98%. We performed a final mapping of all metagenomes on the dereplicated MAGs to calculate their mean coverage and detection. A scheme of the bioinformatics pipeline is provided in Additional File 1.

For phylogenomic analyses we searched and aligned 120 bacterial marker genes of the MAGs using the identity and align commands of GTDB-Tk v1.1.0 [42]. We filtered closely related GTDB taxa identified with the classify_wf workflow with the taxa-filter option during the alignment step. We trimmed multiple sequence alignment using trimAl v1.4.1 [43] with the setting '-gt 0.5' to remove positions with gaps in more than 50% of sequences. We reconstructed a Maximum Likelihood (ML) phylogenetic tree using IQ-TREE v1.6.12 [44] with the 'WAG' general matrix model [45] and 1000 bootstrap replicates that we visualized using anvi'o and FigTree (v1.4.4). Finally, we afforded a finer GTDB reference taxa filtration after a first vizualisation to best represent our MAGs genera. For that purpose, we removed references from distant families and added some from closest genera or families in a supervised manner.

We calculated Average Nucleotide Identity (ANI) online using the ANI calculator (https://www.ezbiocloud.net/tools/ani) [46] As for functional analyses, we extracted KO assignations from anvi'o database for each MAGs and used KEGG-Decoder (www.github.com/bjtully/BioData/tree/master/KEGGDecoder) [47] to determine the completeness of various metabolic pathways. In addition, we used the RAST platform to infer functions of contigs from bins identified as *Zetaproteobacteria* for a finer scale analysis. The metagenome raw reads are available at DOI (10.12770/4186eeef-32b1-4ffb-9a40-61a02a3852b7) and in the European Nucleotide Archive under Bioproject Accession Number PRJEB37577.

Fluorescence In Situ hybridization procedures

We realized FISH procedures as described by Durand et al. 2010. Briefly, we hybridized 0.6 µm transverse sections using Zeta123-Cy5 probe (5'- ACTGATGGGCAGGTAACCACG-3', [23]) directed toward *Zetaproteobacteria*, and EPSI549-Cy3 probe (5'-CAGTGATTCCGAGTAACG-3', [48]) directed toward *Campylobacteria*, together with DAPI staining for cell nucleus observation. Hybridization procedures were fixed at 35 °C and 55% formamide as in [16]. Non-sense probes were tested and gave no signal. We used an Apotome AxioImager Z2 equiped with the COLIBRI led system (Zeiss, Göttingen) for observations.

Results

A highly diverse epibiont community in Rimicaris

We yielded 22–119 million paired-end sequences from shotgun sequencing of total community DNA recovered from the cephalothorax of six *R. exoculata* individuals (RE3, RE5, RE6, RE7, RE12, RE13). Metagenomic assembly of each site yielded 34K–64K contigs longer than 1 kbp, which recruited 14–92% of the raw sequencing reads. Additional File 2 reports statistics for the raw number of reads, quality trimming, filtering, assembly and recruitment results for each sample.

We clustered contigs with respect to their sequence composition signatures and differential coverage patterns across the 6 *Rimicaris* specimens. This binning approach allowed the metagenomic assembly to efficiently segregate into 29 genome bins for Rainbow and 21 for TAG; we retained bins with more than 2 Mbp or more than 60% completion and less than 10% contamination based on the single occurrence of 139 single-copy core genes (SCG) from the collection of [49] implemented in anvi'o [35].

Dereplication (an alignment fraction between genomes of both 0.10 or 0.75) generated a single cluster containing TAG_MAG_00006 and RB_MAG_00023 *Desulfocapsa* (*Desulfocapsaceae*), with lower scores for the latter that was then excluded, resulting in a final collection of 49 MAGs further analyzed (Fig. 2). We nevertheless note that the 49 MAGs reconstructed and described herein represent part of the *Rimicaris* cephalothorax diversity only, and that some remaining groups might be misrepresented given the fact strain diversity can result in assembly breaks and therefore impair binning and recruitment analyses.

Of note, we were unable to reconstruct bacterial MAG (Metagenome-Assembled genome) for Snake Pit using these criteria, due to a much lower sequencing depth for shrimp samples from this site in comparison to Rainbow and TAG ones. MAG collections for TAG and Rainbow, with estimates of completion and redundancy, total bin length, and taxonomic affiliation determined by GTDB are provided in Additional File 3.

We used read mapping against those newly reconstructed genomes to estimate symbiont relative abundance. The actual numbers of reads obtained for each site, that is 75 to 105 million and 111 to 119 millions at TAG and Rainbow, respectively, were homogeneous, allowing for site coverage comparison.

Highly similar symbionts co-exist in single host individuals at both sites

Taking into account the semi quantitative nature of our data, we focused our distribution analyses according to vent origin on the 10 most abundant genome bins. We compared the relative abundance of the four most abundant MAGs at Rainbow (> 100X in at least one Rainbow shrimp) and the six most abundant MAGs at TAG (> 200X in one or both TAG shrimps).

We observed few specific symbionts taking over at distinct hydrothermal vent sites. RB_MAG_00015, *Sulfurovaceae*, was highly abundant at Rainbow (> 295X) while at relatively low coverage at TAG (25X at max). Similarly, we observed RB_MAG_00011, *Sulfurimonadaceae*, was in high abundance at shrimps from Rainbow (104-114X) and with low coverage values at TAG (0.4X maximum). TAG_MAG_00007 (Candidatus *Patescibacteria* phylum, *Paceibacteria* class, from the candidate phyla radiation CPR, Hug et al. 2016) was in high abundance at TAG (205X-361X) but was almost absent at Rainbow (0.5X). TAG_MAG_00018, from the same phylum (*Gracilibacteria* class) was in high abundance at TAG (273X) while in low abundance at Rainbow (max 10X; Additional File 4). The predominance of these groups in the *Rimicaris* holobiont, associated with small genome size for both TAG_MAG_00007 and TAG_MAG_00018 (1,201735 and 841,694 bp, respectively) adds to recent studies showing widespread CPR organisms often in association with abundant autotrophic taxa involved in nitrogen, sulfur and iron cycling [51, 52].

On the other hand, we observed several MAGs abundant at both sites. TAG_MAG_00006, *Desulfocapsa* (*Desulfocapsaceae*) was in great abundance at both Rainbow (167-268X) and TAG (114-242X). Similarly, RB_MAG_00001, assigned to *Flavobacteriaceae* was highly abundant in shrimps from both Rainbow (> 156X) and TAG (18-64X). TAG_MAG_00015, *Alphaproteobacteria Marinosulfonomonas* sp. (*Rhodobacteraceae* family) was the most abundant of all MAGs; it was in extremely high abundance at TAG (180-1273X) while it was also present at Rainbow (10-33X). Interestingly, another *Marinosulfonomonas* sp, RB_MAG_00014, was in high abundance at TAG (69-453X) and was present but in less abundance at Rainbow (19-63X).

Similarly, RB_MAG_00025 (*Thiotrichaceae*) was highly abundant at both Rainbow (551-858X) and TAG (261-321X). TAG_MAG_00019 from the same family was also in high abundance in both TAG (489-598X) and Rainbow (276-426X) shrimps. These data provide further evidence for the occurrence of similar genomes in each host individuals.

A high diversity of metabolic potential among Rimicaris epibionts

Based on the 49 obtained MAGs, we identified the following capabilities in the shrimp microbiome. Figure 3 illustrates this potential metabolic plasticity among symbiotic lineages.

Autotrophic Carbon Fixation

Eight MAGs belonging to *Gamma*, *Zeta* and *Alphaproteobacteria* showed the capacity to fix carbon though the CBB cycle at both sites (Fig. 3). In contrast, only the two *Campylobacteria Sulfurovaceae* MAGs from Rainbow and TAG harbored the complete set of genes for the rTCA cycle. The *Deltaproteobacteria Desulfocapsaceae* MAGS were the only ones harboring the Wood-Ljungdahl pathway genes for carbon assimilation at both TAG and Rainbow.

Glycolysis, Tca Cycle And Heterotrophy

Almost all MAGs had the capacity for glycolysis and 43 showed the potential for the TCA cycle. We noted the potential for carbon degradation and heterotrophic capacities in 35 MAGs from both sites using glucoamylase (1MAG), D-galacturonate epimerase (20 MAGs), D-galacturonate isomerase (4 MAGs), chitinase (5 MAGs), beta-N-acetylhexosaminidase (22 MAGs), beta-glucosidase (1 MAG) and pullulanase enzymes (6 MAGs). Of note, chitinases could be used to graze on chitin degrading shrimp molts under heterotrophic metabolisms but bacteria can also secrete them during pathogenesis and symbiosis for cell adhesion [53].

Mixed Acid Fermentation

An important diversity of MAGs from both TAG and Rainbow sites may have the capacity for mixed acid fermentation (conversion of pyruvate to fermentation products) including pyruvate to lactate (1 MAG), pyruvate to formate + Acetyl-CoA (20 MAGs), formate to CO_2 & H_2 (18 MAGs), to acetate (8MAGs, including *Flavobacteriaceae*), to ethanol (2 MAGs) and phosphoenolpyruvate (PEP) to succinate via oxaloacetic acid

(OAA), malate & fumarate (41 MAGs including *Sulfurovaceae*). Of note, many of these pathways were nevertheless incomplete.

Sulfur Metabolism

Dissimilatory sulfate reduction. The *sat* genes for ATP sulfurylase were identified in 12 MAGs from both sites while the *apr*AB genes for adenosine phosphosulfate reductase and the *dsr* genes for dissimilatory sulfite reductase were found in 4 and 9 of those, respectively.

SOX system. 12 MAGS from both TAG and Rainbow were observed as capable of thiosulfate oxidation (using *sox* genes). The capacity for alternative thiosulfate oxidation (*tsdA* genes) was found in *Sulfurocaceae* MAGS from both sites. Thiosulfate polysulfide reductase (reverse), possibly converting thiosulfate into sulfite and hydrogen sulfide was identified in 10 MAGs. We also identified the *sor* genes in

10 MAGs and the *soe* genes in 8 MAGs. The capacity for sulfide oxidation using *sqr* genes was found in 25 MAGS. The *dms* genes (for DMSO reductase) were identified in 9 MAGs.

Hydrogen Metabolism

The *hox* genes for NAD-reducing hydrogenase were identified in 6 MAGs from both sites and a total of 18 MAGs encoded the *hyd* genes for the NiFe hydrogenase.

Nitrogen Metabolism

Denitrification. The potential for dissimilatory nitrate reduction using *nar* or *nap* genes were identified 15 MAGS from both sites. In addition, the capacity for the denitrification step of nitrite reduction requiring *nir* genes was observed in 14 MAGs, the one of nitric oxide reduction requiring *nor* genes in 19 and the one of nitrous-oxide reduction requiring *nos* genes in 18 similar and additional MAGs.

DNRA. Dissimilatory nitrate reduction to ammonium (DNRA) requiring *nir* or *nrf* genes were retrieved in 6 MAGs.

Nitrification. The key enzyme for nitrite oxidation, nitrite oxidoreductase (NXR) was identified in 6 MAGs. In addition, nitrogen fixation (using *nif* genes) were retrieved in the two *Desulfocapsaceae* MAGs only, congruent with the recent study of Jiang et al. 2020.

Oxygen Sensing

Genes for Cytochrome.c.oxidase (*cox*), ubiquinol.cytochrome.c.reductase (*pet*;*fbc*), Cytochrome.c.oxidase.cbb3.type (*cco*) *and* Cytochrome.bd.complex (*cyd*), which show different affinities for oxygen, were respectively found in 18, 12, 29 and 22 MAGs from both sites.

Symbiont-host Colonization

The capacity for biofilm exopolysaccharide PGA synthesis was identified in one *Desulfocapsaceae* MAG only and the potential for sulfolipid biosynthesis was identified in one MAG from the *Trueperaceae* family. In addition, we observed an enrichment of genes coding for secretion systems from Type I within 11 MAGs from the *Rhodobacteraceae*, *Flavobacteriaceae*, and *Marinicellaceae* families. Type II encoding pili-related proteins were also observed in 18 MAGS. Overall, Type I and Type II mediate the secretion of a large variety of protein substrates (unfolded and folded) often associated with virulence [54, 55] that could be used by symbionts to colonize hosts. Virulence factors such as hemolysins and chitinases exported by type II secretion system have been shown to be critical for initial establishment of symbiont *Aeromonas veronii* in the leech gut [56] or in the active invasion of the rice fungus *Rhizopus microsporus*

by its endosymbionts *Burkholderia rhizoxinica* [57]. Type III secretion systems was possibly identified in one *Mariprofundaceae* MAG only, yet not all genes subunits were retrieved. These secretion systems are usually found in pathogenic bacteria, promoting the transfer of bacterial effector proteins to eukaryotic cells and promoting bacterial invasion and colonization [54, 55]. Type IV secretion systems, possibly involved in the dissemination of mobile genetic elements in addition to effector molecules were solely found in *Rhodobacteraceae* (4 MAGs) and *Flavobacteriaceae* (1 MAG) at both TAG and Rainbow. These secretion systems also encode pili that enable directional crawling (twitching motility), biofilm formation and adhesion at the initial colonization steps. Type VI secretion systems were observed in the same *Rhodobacteraceae* MAGs as Type IV. These secretion systems are reported to transfer toxic effector proteins into eukaryotic and prokaryotic target cells and having important role in pathogenesis and to defend bacteria against competing organisms [53]. Noteworthy, twin Arginine Targeting (Tat) systems, other bacterial secretion systems documented to transport fully folded protein substrates and being vital to bacteria [58], were identified in 36 MAGs.

Detoxification

Cobalt transporters (*cbi* and *cor* genes) were identified in 5 and 4 MAGs, respectively belonging to *Desulfocapsaceae* and *Sulfurimonadaceae*. Copper transporters and ferrous iron transporters were found in 15 and 27 MAGS, respectively. Striking, a total of 41 MAGs showed the potential for arsenic reduction.

Vitamins, Amino Acids Biosynthesis And Transporters

A total of 48 MAGs showed the capacity to encode some of the genes required for thiamin biosynthesis and 37 could synthesize riboflavin and cobalamin, suggesting the importance of vitamin synthesis for the epibiont community. In addition, the presence of thiamin transporters in 9 MAGS confirmed the capacity to export newly synthesized vitamins. Input substrates like AcetylcoA and pyruvate for the biosynthetis of essential amino acids such as Lysine and Isoleucine [59] were found in at least 41 MAGS. In addition, the presence of genes coding for phosphate transporters in 24 MAGs across more than 6 families suggest the capacity and importance of phosphate uptake in the *Rimicaris* holobiont.

Flagellum & Chemotaxis

Flagellum biosynthesis was identified in 13 MAGs belonging to *Rhodobacteraceae Desulfocapsaceae*, *Melioribacteraceae*, *Sulfurimonadaceae* and *Mariprofundaceae*.The capacity for chemotaxis was identified in 19 MAGs belonging to the same families.

A high diversity of novel lineages that lack representative genomes

To infer how symbiotic genomes reconstructed in this study are distributed relative to known taxa, we afforded a phylogenomic analysis using our 49 MAGs as well as 600 closely related genomes from GTDB (Fig. 4A). The ML tree based on concatenated marker proteins showed 49 MAGs spanning 9 divergent phyla, that is, an important phylogenetic diversity. Nevertheless, MAGs covered only 10 known genera while the majority are family-level branches, showing the importance of lineages lacking representatives and important epibiont diversification.

Two newly reconstructed Zetaproteobacteria MAGs co-occur at both sites

We estimated that *Zetaproteobacteria* lineage represented between 0.1–0.3% of total bacteria in our *Rimicaris* DNA extracted samples using qPCR, suggesting that our DNA extraction protocol was well suited for some of the most cumbersome symbionts.

One *Zetaproteobacteria* MAG (hereafter, referred to as RB_MAG_00008, 168 splits; 1,853,475 bp; 92.96% complete and 2.82% contamination) had a low coverage at both sites (maximum 29X and 17 X at Rainbow and TAG, respectively) while another one (hereafter TAG_MAG_00014, 204 splits contigs; 1,625,457 bp, 94.37.1% complete and 2.82% contamination) was more represented at TAG (19-155X) than at Rainbow (max 2.5X). Using FISH procedures, we could observe cells as small rods, curved and closely attached to the host cuticule, usually under the long filamentous *Campylobacteria* symbionts (Fig. 5). This observation is in agreement with TEM observations done [28]. Unfortunately, MAGs data did not allow recovering 16S rDNA genes to design specific probes for each symbiont, nor did previous studies leading to a single lineage sequence [12, 16] and unpublished data. We therefore could not yet fully describe the distribution of both recovered *Zetaproteobacteria* related MAGs. Both RB-MAG-00008 and TAG-MAG-00014 were found as divergent, yet close relatives to *Ghiorsea bivora* isolated from TAG (Fig. 4B) [25].

As KEGG decoder predicts the completeness of pathways based on the presence of a set of key genes, we attempted validating these findings and a more detailed analysis of the different *Zetaproteobacteria* genomes (from this study and their free-living counterparts) using RAST and FeGenie. Regarding carbon cycle, although both MAGs were incomplete, the presence of key enzyme for the CBB cycle (i.e., Rubisco: ribulose bisphosphate carboxylase) in both *Zetaproteobacteria* MAGs confirmed the possibility of autotrophic carbon assimilation in these host-associated lineages (Fig. 3). Both have the FormII Rubisco (*cbbl* gene), which is in agreement with their symbiotic life under external seawater flow with relatively low oxygen and high carbon dioxide content [10]. In addition, even if fully described as autotrophic bacteria under culturing approaches, *Zetaproteobacteria* also share genes of the TCA cycle, suggesting possible mixotrophy [24, 26]. Here, the potential for carbon degradation using beta-N-acetylhexosaminidase enzyme retrieved in both MAGs and genes for mix acid acetate production found in RB_MAG_00008 suggests a putative heterotrophic behavior.

Both strains seem capable of using several electron donors. A sulfide:quinone oxidoreductase *sqr* in both bins and of adenylyltransferase *sat* in RB_MAG_00008 (Table 1) suggest they are capable of sulfur oxidation. In addition, the presence of NiFe-hydrogenase I cytochrome b subunit as well as *Hox* and *Hyp* genes in RB_MAG_00008 suggests hydrogen could also potentially sustain this symbiosis, like for their closest relative *Ghiorsea bivora* [25]. As for iron oxidation, *Cyc2* genes were retrieved in both MAGs using FeGenie, confirming they have the potential to oxidize Fe (II) [25, 60] (See additional File 5). Cbb3-type cytochrome c oxidase encoding genes, involved in oxygen sensing and detoxication [26] but also in the process of aerobic, neutrophilic Fe oxidation and highly expressed in cultivated *Mariprofundus ferrooxydans* PV-1 were also found in both bins [60]. Further, genes coding for multicopper oxidase (MCO), potentially also involved in Fe(II)-oxidation [61] were found in RB_MAG_00008 (data not shown).

Both MAGs show genes implied in dissimilatory nitrate reduction to ammonium (DNRA) suggesting ability of nitrogen acquisition, like their closest relative [25]. Glutamine synthetase and glutamate synthase enzyme were also encoded in both bins, suggesting that ammonia could be incorporated into amino acids, may it come from nitrate reduction or environmental uptake, and that the symbionts may then have the potential to recycle ammonium host's waste. We also identified genes coding for ABC transporter ATP binding proteins, ABC transporter, substrate-binding protein, and ABC transporters permeases (data not shown), used for the transport of amino acids after biosynthesis in both MAGs. The presence of genes for thiamin, riboflavin and cobalamin biosynthesis also indicate both MAGs probably have the ability to vitamins synthesis.

Numerous genes usually implied in host symbiont interactions are present. Occurrence of genes coding for arsenical resistance proteins suggest the symbionts have the genetic potential for arsenic detoxification that might benefit the shrimps. We observed Type II secretion systems, as well as phosphate and copper transporters in each MAG suggesting they can transport proteins (including potential bacterial toxins and degradative enzymes such as proteases and lipases), ions and metals. In addition, the presence of exopolyphosphatases and polyphosphate kinase in both MAGs, suggest they are capable of producing polyphosphate, in agreement with previous observations [10, 16, 26]. The presence of transcriptional regulator from the *LuxR* family in RB_MAG_00008 suggests a link with Quorum Sensing (QS), which might allow bacteria to communicate and play a crucial role in symbiosis, such as sustaining biofilm on the host [62]. Both MAGs also contained the two-component transcriptional response regulator, OmpR family, reported to play important role in bacterial infection in other deep-sea symbiosis [53]. Finally, genes encoding flagella and chemotaxis were encoded in both symbiotic MAGs. In particular, we observed that numerous flagella biosynthesis encoding genes including hook-associated *Flg* (BCGIJK) genes, possibly from the same operon [63], as well as flagellar rotation genes *mot* (AB) were present in both bins.

Overall, the lack of hydrogen oxidation as well as QS genes in TAG_MAG_00014 suggests not random gene gain and loss between both MAGs and a putative signature of divergent niche and functions. ANI values of 88.74% between both *Zetaproteobacteria* MAGS, and of less than 77% between RB_MAG_00008 or TAG_MAG_00014 and their closest relative, *Ghiorsea bivora* from TAG site, confirmed

the presence of distinct *Rimicaris*-associated *Zetaproteobacteria* species, divergent from their free-living counterparts.

Discussion

In this study, we used metagenomic data of *Rimicaris exoculata* shrimps epibiont communities from three contrasting hydrothermal sites along the Mid-Atlantic Ridge to reconstruct genomes and examine functional potential at the genome-resolved scale. We recovered 49 high-quality MAGs from TAG and Rainbow sites. Although no MAG was reconstructed from the chemically contrasting site Snake Pit, it proved informative, providing differential coverage values that improved the binning strategy.

Possible synthrophy among metabolically diversified Rimicaris epibionts

Overall, we observed *Rimicaris* symbionts have genomes with considerable functional diversity. The potential for autotrophic growth was observed in 10 out of the 49 MAGs. Eight of those ten MAGs, belonging to *Gamma*, *Zeta* and *Alphaproteobacteria* contained the complete set of genes for the CBB cycles, and our data confirmed that the *Sulfurovaceae* MAGs were the sole capable of mediating chemoautotrophy through the rTCA cycle. The presence of both rTCA and CBB cycles in *Rimicaris* epibiont community was already reported [12, 16], suggesting it might allow the consortium to switch cycle depending on environmental conditions with balanced level of oxygen and carbon dioxide. The rTCA cycle, harboring oxygen-sentivive enzymes, is supposedly more adapted to more anoxic conditions together with higher temperatures, and is energetically more favorable than the CBB cycle [14, 64]. This property might partly explains the *Campylobacteria* success in these environments. In addition, the *Deltaproteobacteria Desulfocapsaceae* MAGs from both Rainbow and TAG sites were shown to possess genes for the Wood-Ljungdahl pathway, allowing the use of hydrogen as electron donor and carbon dioxide as both electron acceptor and for biosynthesis, confirming the recent findings of [15].

Our data also unravel the complexity of this symbiotic consortium with heterotrophic capabilities in 35 MAGs (including the *Rhodobacteraceae*, *Desulfocapsaceae*, *Flavobacteriaceae, Melioribacteraceae*, *Sulfurimonadaceae* and *Sulfurovaceae* families Fig. 3). Among those MAGs, a high number then showed the capacity to perform mixed acid fermentation. In addition, some actually featured genes for both heterotrophic and autotrophic behaviors, like the *Sulfurovaceae* family. A mixotrophophic mode of *Campylobacteria* (formerly *Epsilonproteobacteria*) was previously suggested as a way for symbionts to potentially cooperate with heterotroph [17]. Not only fueling their host, bacterial lineages may also undergo syntrophic relationships. *Campylobacteria* have been shown to produce exopolysaccharide mats through autotrophic pathway [65], thus providing an attachment surface as well as a source of organic matter that can offer a new niche to heterotrophic bacteria such as *Bacteroidetes*. As a response, heterotrophic *Bacteroidetes* are able to produce organic matter including acetate. The latter can then be utilized back as a carbon source by *Campylobacteria* [17], as they also have potential to grow heterotrophically by incorporating acetate with an Acetyl CoA synthetase [66]. Although current data are based on the presence of genes and therefore indicate potential functions only, expression analyses of

the newly reconstructed MAGs in controlled conditions would allow validating a synthophy hypothesis between *Rimicaris* epibionts. These results however add to previous work suggesting a high metabolic plasticity that might confer an adaptive advantage for these epibionts in the highly dynamic hydrothermal gradients they thrive in. In return, it may provide an obvious advantage for their host, which could explain its observed success in colonizing vent fluids that vary in composition and concentration.

We further investigated which energy sources potentially powered those symbioses, and observed that 32 MAGs (that is, more than half of the population) showed genes related to sulfur metabolism through a diversity of genes (including *sat*, *apr*, *dsr*, *sox*, and *sqr*). 17 MAGs showed the potential for hydrogen oxidation, confirming the importance of H_2 as an electron donor for the *Rimicaris* symbiosis, probably participating to its success at Rainbow where sulfide is lower. Finally, two *Zetaproteobacteria* MAGs may oxidize iron, as further developed below. We observed 29 MAGs encoding the cbb3-type cytochrome c oxidase enzyme, used for sensing and respiration with oxygen as electron acceptor but also for protection against oxidative stress. Four MAGs (belonging to *Rhodobacteraceae* and *Marinicellaceae* families) showed possible use of an alternative electron acceptor than oxygen such as nitrate, which encoded all the genes required for the complete reduction of nitrate to dinitrogen. Although the gene coding for nitrate reductase was lacking in *Campylobacteria*, possibly due to incomplete genome bins, the presence of three other denitrification genes suggest it could also potentially use nitrate, as described by [16]. Apart from these, 30 additional MAGs encoded some of the enzymes involved in nitrogen metabolism. Members of families like *Rhodobacteraceae* seemed to possess the capacity for denitrification, DNRA, and nitrification, which may provide them with some more metabolic flexibility as compared to more specialist taxa.

An Arsenal Of Genes For Host-symbiont Colonization And Interaction

In addition, because the episymbionts have the potential to synthesize and transport vitamins, such as thiamin, riboflavin and cobalamin, the nutritional advantages for the host may go beyond a rich source of carbon and energy. The presence of genes for the biosynthesis of energy storage compounds, like polyphosphate, supports previous results showing polyphosphate- granules in the *R. exoculata* holobiont as well as in *M. ferrooxydans* cells [10, 26] and the genomic potential for their synthesis [16]. It was suggested the polyphosphate granules serve as phosphorus and energy storage that may help the shrimps, thriving around the vent fluid emission to cope with varying environmental conditions [16]. Further, a total of 41 MAGS did show genes involved in arsenic reduction, which suggested a potential role of detoxification, useful for the holobiont (the host, its associated microbes and their interactions). The presence of high concentration of Arsenic, highly correlated with Zinc, was reported along the Mid-Atlantic Ridge [67].

Finally, each ten days, adults undergo molt even, which necessitate permanent and controlled microbiote colonization processes. Among them, secretion systems and biofilm formation are considered as central

in host symbiont recognition. In line with this, the majority of MAGs (43) share characteristics of pathogens and beneficial microbes through genes encoding secretion systems (the general type I-VI and a striking number of Twin targeting system or Tat) and biofilm formation that might facilitate their success while colonizing the host.

Dual Zetaproteobacteria **symbiosis in** Rimicaris: **candidatus** Ghiorsea rimicarensis **and Candidatus** Ghiorsea crypta

Two distinct highly complete *Zetaproteobacteria* symbiotic genomes, of 1.6 to 1.8 Mbp, were for the first time recovered at both TAG and Rainbow sites. Previously sampled Rainbow *R. exoculata* individuals showed *Zetaproteobacteria* using Fluorescence *In Situ* Hybridization [16] (Fig. 2), yet their genomic potential and a potential microdiversity remained hidden. Here, we confirmed these findings using a similar FISH procedure (Fig. 5) and show both lineages are closely related to *Ghiorsea bivora* [25] isolated from TAG vent site, although they differ between each other.

The genetic possibility that these epibionts oxidize iron as suggested by several authors [3, 4, 10, 16, 27, 28] was reinforced herein for the first time using canonical *cyc2* iron oxidizing genes. Of note, *cyc2* genes showed a slightly different average coverage as compared to the remaining *Zetaproteobacteria* genes (data not shown). These data could imply environmental populations with high level of strain heterogeneity, as described in [68]. In line with this, it is possible that these genes are present on extrachromosomal elements, which were not reconstructed herein and in previous studies, and explaining the reported difficulty to retrieve those genes in Fe(II) oxydizers [40]. The presence of a plasmid in the *Wolbachia* endosymbiont from *Culex pipiens* mosquitoes was first identified following similar distinct coverage signature as compared to bacterial genes in ovaries metagenomes [69].

Further, as their closest cultivated counterpart *G. bivora*, both MAGs had the complete set of genes to fix carbon though the CBB cycle. The presence of genes for heterotrophic behavior also suggest they may be able of mixotrophy, as proposed before by Singer and colleagues [26] for *M. profundus* PV1. Still, mixotrophic growth was not confirmed through cultural approaches [19, 25]. The ability to use sulfur (for example using *sqr* genes), in addition to H_2 and Fe(II) as shown for *G. bivora* further expend the metabolic repertoire of the *Zetaproteobacteria*. Nevertheless, we observed striking differences between both MAGs, such as the capacity for hydrogen oxidation and sulfur oxidation using additional adenylyltransferase *sat* genes retrieved in RB_MAG_00008 only. This may contribute to niche partitioning between both symbionts, giving them more flexibility according to environmental condition variations and avoiding possible competition. In line with this, the presence of *LuxR* family transcription factors in RB_MAG_00008 suggests molecular conversations within the *Rimicaris* hobiont via Quorum Sensing. These data adds to previous work highlighting QS mechanisms controlling the regulation of the *Rimicaris* Campylobacterial and Gammaproteobacterial symbionts growth and proliferation as well as the bacterial selection from the microbial environmental pool [62]. Regarding additional host-Zetaproteobacterial symbiont recognition and colonization, suggested to occur each ten days along molt cycle, the presence of flagellar and chemotaxis genes in both MAGs also suggest they are able to actively move toward

favorable environments, including host sensing signals. The squid-vibrio symbiosis show distinct flagellar functions ranging from swimming capacity to chemotaxis and host signaling and communication, which suggest essential and constitutive roles for these structures [70]. It is possible flagella identified in free-living closest relative *G. bivora* [25] is also used here for host symbiont colonization. Further, the *Zetaproteobacteria* MAG RB-MAG-0008 showed genes coding for multicopper oxidase (MCO) which were shown as potential homologs for iron oxidation in several other taxa oxidizing iron [61]. Fragmentation due to the co-assembly of closely related bacterial strains in these diverse environments and incomplete genomes could explain that some pangenomic traits are absent from some metagenomic bins. Yet, the lack of random patterns, that is the absence of several genes coding for hydrogen oxidation together with QS in RB_MAG_00008, suggest some distinct lifestyles for each MAG allowing them to select different niches.

The two *Zetaproteobacteria* MAGs showed substrates for amino acids synthesis and their transport adding to previous data showing *Rimicaris* epibionts can synthesize and transport amino acids. The recently reconstructed Candidatus *Desulfobulbus rimicarensis* (Deltaproteobacterial) from *Rimicaris*, proved capable of synthesizing all 20 amino acids, with all the genes essential for amino acid biosynthesis present in the genome and expressed [15]. These results stress the important rate and role of transfers within the *Rimicaris* holobiont. Overall, these data contrast with other symbiotic system like *Bathymodiolus thermophiles* of the vent mussel, *Riftia pachyptila* or *Calyptogena magnifica*, where host lysis of its symbionts plays a more important role in the nutrition of the hosts, as highlighted by significant protein-degrading activity [71].

RB_MAG_00008, estimated with a genome size of 1,853,475 bp and 92.96% completion based on the presence of single copy core genes [49], suggests an actual genome of around 2 Mb. On the contrary, a reconstructed genome size of ca. 1,625,457 bb and 94.37% completion for TAG_MAG_00014 suggests an actual genome size of ca. 1, 7 Mbp, that is, a slightly reduced and presumably streamlined genome. Nevertheless, this is to our knowledge the first study to report symbiotic *Zetaproteobacteria* genomes. Based on Average Nucleotide Identity (ANI) values of 89.74% between two newly reconstructed *Zetaproteobacteria* MAGs and less than 77% with their closest relatives *Ghiorsea bivora* from TAG, we propose they belong to potential novel species [72]. We suggest the names of Candidatus *Ghiorsea rimicarensis for* RB_MAG_00008 and Candidatus *Ghiorsea crypta for* TAG_MAG_00014. Differential average coverage for the two lineages could then suggest that specific *Zetaproteobacteria* lineages take over, at distinct or within a single hydrothermal vent site, depending on the environmental conditions. Surprisingly, the number of *Zetaproteobacteria* was higher at TAG, where *G. bivora* was also isolated [25] than at the iron richer site Rainbow. This may be due to some more robust iron incrustations for Rainbow specimens, despite the use of a thorough DNA extraction protocol herein.

Niche partitioning in the Rimicaris **holobiont**

As for *Zetaproteobacteria*, two highly similar MAGs (*Thiotrichaceae* RB_MAG_00025 and TAG_MAG_00019) were found at both Rainbow and TAG, and two *Marinosulfonomonas* MAGs

(TAG_MAG_00015 and RB_MAG_00014) were found in varying abundance at both sites. Genes for the glycolyse, dissimilatory nitrate reduction and thiosulfate oxidation were present in both *Thiotrichaceae* symbiont populations. Nevertheless, enzymes for nitric oxide reduction, NiFe hydrogenase Hyd-1 and dissimilatory sulfate reduction were encoded only in TAG_MAG_00019 while the ones for dissimilatory sulfite reduction and sulfide oxidation was solely encoded in RB_MAG_00025. The observed functional differences between the closely related *Thiotrichaceae* MAGs could suggest some complementary rather than competitive strains and may explain their co-occurence. It is also possible one *Thiotrichaceae* strain performs some of the dissimilatory sulfate metabolic steps and that the other covers the remaining ones. Likewise, both *Marinosulfonomonas* sp MAGs RB_MAG_00014 and TAG_MAG_00015 have the potential for the glycolyse, the fixation of carbon using the CBB cycle, partial to complete reduction of nitrate to dinitrogen (N_2), respectively, as well as sulfide and hydrogen oxidation (Fig. 3). Nevertheless, only TAG_MAG_00015 showed genes for both the complete oxidation of nitrate to N_2, and DNRA genes, among others. On the other hand, no *Marinosulfonomonas* sp seemed able to utilize CH_4, suggesting strains with different metabolic pathways than the ones described by Holmes et al. [73], putatively constrained by their association with animal hosts. Overall, we observed behind an apparent functional redundancy, an important symbiont strain diversity that possibly have great implications for the functioning of the complex *Rimicaris* symbiosis. These data are congruent with recent studies showing genomic heterogeneity in vent mussel symbiont population that either possess or lack a key gene cluster, suggesting specialized rather than generalist symbionts [74, 75]. The diversity of *Rimicaris* MAGs capable of sulfur oxidation is in agreement with previous work describing more than 16 different sulfur oxidizer strains in four *Bathymodiolus* species from the Mid-Atlantic Ridge and showing an important adaptability to the holobiont in vents [74]. These seemingly closely related strains were suggested to differ in key functions including the use of energy and nutrient sources, viral defense genes and electron acceptors. Authors suggest that some animals may have a higher tolerance than previously thought to maintain “less efficient” strains among “more efficient” ones as the cost for their maintenance is limited [74]. In other words, these different studies posit the costs for the maintenance of such symbiont diversity may be counterbalanced by the plasticity it offers, that is, a larger adaptability and resilience, especially in these unstable environments. In addition to obvious functional differences, it is likely more subtle phenetic differences such as a better adaptation to temperature or pressure, allowing each of these strains to occupy and be adapted to different micro-niches. High levels of strain variability and numerous ortholog key proteins in vent-associated polychaete worm *Alvinella pompejana* were hypothesized as being each optimally adapted to thermal fluctuations within the worm habitat [76]. Similarly, Alcaide and colleagues [77] suggested diverse carboxyl esterases of the gill-associated microbiota form *Rimicaris* may reflect distinct habitat-specific adaptations. Although it was not possible to determine whether geochemical or thermal fluctuations impose selection pressures on the epibiont community, this study adds to previous work that symbiont genetic diversity is more widespread than currently appreciated and that it might underpin ecosystem functioning and resilience in the highly dynamic hydrothermal vents.

Conclusions

These data unravel a much more complex microbial consortium associated within *R. exoculata* than previously appreciated and highlight some generalized niche partitioning between symbionts. It stresses the apparent functional redundancy at the genome-wide level between co-existing strains hides differences that may reflect distinct history traits. This may be the key of this holobiont success along the Mid Atlantic Ridge, encountering contrasted habitats and able of large connectivity [78]. Two Zetaproteobacterial symbionts add to the metabolic catalogue shared by the *Rimicaris* holobiont and to the repertoire of metabolic diversity and Lifestyle of the *Zetaproteobacteria*. Taken together, our results reveal highly complex symbioses giving new insights into deep-sea ecosystems functioning and resilience, may they be threatened by anthropogenic or natural issues.

Declarations

Acknowledgements

We thank cruise chief scientists of MOMAR2008-Leg2, Biobaz 2013 and BICOSE 2014 (J. Dyment, F. Lallier and M.A. Cambon-Bonavita) and the captains and crew of R/Vs *Pourquoi pas?* and Atalante and ROV Victor for logistic assistance in collecting samples. We also thank Cyrielle Jan for FISH experiments and pictures, Hilary Morrison for assistance with sequencing and A. Murat Eren for helpful comments on the manuscript.

Funding

Funding was provided by Ifremer REMIMA program, and LabexMer post-doctoral fellowship from the University of Western Brittany.

Authors' information

Affiliations

Ifremer, Univ Brest, CNRS, Laboratoire de Microbiologie des Environnements Extrêmes, UMR6197, 29280 Plouzané, France

Marie-Anne Cambon-Bonavita, Johanne Aubé, Valérie Cueff-Gauchard, Julie Reveillaud

DGIMI, Univ Montpellier, INRA, F-34095 Montpellier, France

Julie Reveillaud

Authors' contributions

MAC interpreted the data and wrote the manuscript. JA analyzed the data and prepared the figures. VCG organized samples and performed laboratory assays. JR performed laboratory assays, analyzed the data, wrote the manuscript and supervised the project. All authors read and approved the manuscript.

Corresponding author

Correspondence to Julie Reveillaud

Ethics declarations

Ethics approval and consent to participate

Not applicable

Consent for publication

Not applicable

Availability of data and material

All data generated or analyzed during this study are included in this published article (and its supplementary information files).

Competing interests

The authors declare that they have no competing interests.

References

1. Williams A, Rona P. Two new caridean shrimps (bresiliidae) from a hydrothermal field on the Mid-Atlantic Ridge. J Crustac Biol. 1986;446–62.
2. Segonzac M, de Saint Laurent M, Casanova B. L'enigme du comportement trophique des crevettes Alvinocarididae des sites hydrothermaux de la dorsale medio-Atlantique. Cah Biol Mar. 1993;535–71.
3. Schmidt C, Le Bris N, Gaill F. Interactions of deep-sea vent invertebrates with their environment: the case of *Rimicaris exoculata*. J Shellfish Res. 2008;27:79–90.
4. Zbinden M, Cambon-Bonavita M-A. Occurrence of Deferribacterales and Entomoplasmatales in the deep-sea Alvinocarid shrimp *Rimicaris exoculata* gut. FEMS Microbiol Ecol. 2003;46:23–30.
5. Durand L, Zbinden M, Cueff-Gauchard V, Duperron S, Roussel EG, Shillito B, et al. Microbial diversity associated with the hydrothermal shrimp *Rimicaris exoculata* gut and occurrence of a resident microbial community. FEMS Microbiol Ecol. 2010;71:291–303.
6. Durand L, Roumagnac M, Cueff-Gauchard V, Jan C, Guri M, Tessier C, et al. Biogeographical distribution of *Rimicaris exoculata* resident gut epibiont communities along the Mid-Atlantic Ridge hydrothermal vent sites. FEMS Microbiol Ecol. 2015;91:1–15.
7. Polz MF, Cavanaugh CM. Dominance of one bacterial phylotype at a Mid-Atlantic Ridge hydrothermal vent site. Proc Natl Acad Sci U S A. 1995;92:7232–6.

8. Waite DW, Vanwonterghem I, Rinke C, Parks DH, Zhang Y, Takai K, et al. Comparative genomic analysis of the class Epsilonproteobacteria and proposed reclassification to epsilonbacteraeota (phyl. nov.). Front Microbiol. 2017;8.
9. Waite DW, Vanwonterghem I, Rinke C, Parks DH, Zhang Y, Takai K, et al. Addendum: Comparative genomic analysis of the class Epsilonproteobacteria and proposed reclassification to Epsilonbacteraeota (phyl. nov.). Front Microbiol. 2018;9:1–2.
10. Zbinden M, Shillito B, Le Bris N, de Villardi de Montlaur C, Roussel E, Guyot F, et al. New insights in metabolic diversity among the epibiotic microbial communities of the hydrothermal shrimp *Rimicaris exoculata*. J Exp Mar Bio Ecol. 2008;159:131–40.
11. Petersen JM, Zielinski FU, Pape T, Seifert R, Moraru C, Amann R, et al. Hydrogen is an energy source for hydrothermal vent symbioses. Nature. 2011;476:176–80.
12. Guri M, Durand L, Cueff-Gauchard V, Zbinden M, Crassous P, Shillito B, et al. Acquisition of epibiotic bacteria along the life cycle of the hydrothermal shrimp *Rimicaris exoculata*. ISME J. 2012;6:597–609.
13. Cowart DA, Durand L, Cambon-Bonavita MA, Arnaud-Haond S. Investigation of bacterial communities within the digestive organs of the hydrothermal vent shrimp *Rimicaris exoculata* provide insights into holobiont geographic clustering. PLoS One. 2017;12:1–22.
14. Hügler M, Sievert SM. Beyond the Calvin Cycle: Autotrophic Carbon Fixation in the Ocean. Ann Rev Mar Sci. 2011;3:261–89.
15. Jiang L, Liu X, Dong C, Huang Z, Cambon-Bonavita M-A, Alain K, et al. Candidatus *Desulfobulbus rimicarensis*, an uncultivated deltaproteobacterial epibionts from the deep-sea hydrothermal vent shrimp Rimicaris exoculata. Appl Environ Microbiol. 2020.
16. Jan C, Petersen JM, Werner J, Teeling H, Huang S, Glöckner FO, et al. The gill chamber epibiosis of deep-sea shrimp *Rimicaris exoculata*: An in-depth metagenomic investigation and discovery of Zetaproteobacteria. Environ Microbiol. 2014;16:2723–38.
17. Ponsard J, Cambon-Bonavita M-A, Zbinden M, Lepoint G, Joassin A, Corbari L, et al. Inorganic carbon fixation by chemosynthetic ectosymbionts and nutritional transfers to the hydrothermal vent host-shrimp *Rimicaris exoculata*. ISME J. 2013;7:96–109.
18. Emerson D, Moyer CL. Neutrophilic Fe-oxidizing bacteria are abundant at the Loihi seamount hydrothermal vents and play a major role in Fe oxide deposition. Appl Environ Microbiol. 2002;68:3085.
19. Emerson D, Rentz JA, Lilburn TG, Davis RE, Aldrich H, Chan C, et al. A novel lineage of proteobacteria involved in formation of marine Fe-oxidizing microbial mat communities. PLoS One. 2007;2.
20. Field EK, Sczyrba A, Lyman AE, Harris CC, Woyke T, Stepanauskas R, et al. Genomic insights into the uncultivated marine Zetaproteobacteria at Loihi Seamount. ISME J. 2015;9:857–70.
21. McAllister SM, Moore RM, Gartman A, Luther GW, Emerson D, Chan CS. The Fe(II)-oxidizing Zetaproteobacteria: historical, ecological and genomic perspectives. FEMS Microbiol Ecol. 2019;95:1–18.

22. Scott JJ, Breier JA, Luther GW, Emerson D. Microbial iron mats at the Mid-Atlantic Ridge and evidence that zetaproteobacteria may be restricted to iron-oxidizing marine systems. PLoS One. 2015;10:1–19.
23. Kato S, Yanagawa K, Sunamura M, Takano Y, Ishibashi JI, Kakegawa T, et al. Abundance of Zetaproteobacteria within crustal fluids in back-arc hydrothermal fields of the Southern Mariana Trough. Environ Microbiol. 2009;11:3210–22.
24. Hoshino T, Kuratomi T, Morono Y, Hori T, Oiwane H, Kiyokawa S, et al. Ecophysiology of Zetaproteobacteria associated with shallow hydrothermal iron-oxyhydroxide deposits in Nagahama Bay of Satsuma Iwo-Jima, Japan. Front Microbiol. 2016;6:1–11.
25. Mori JF, Scott JJ, Hager KW, Moyer CL, Küsel K, Emerson D. Physiological and ecological implications of an iron- or hydrogen-oxidizing member of the Zetaproteobacteria, Ghiorsea bivora, gen. nov., sp. Nov. ISME J. 2017;11:2624–36.
26. Singer E, Emerson D, Webb EA, Barco RA, Kuenen JG, Nelson WC, et al. *Mariprofundus ferrooxydans* PV-1 the first genome of a marine Fe(II) oxidizing Zetaproteobacterium. PLoS One. 2011;6.
27. Corbari L, Zbinden M, Cambon-Bonavita MA, Gaill F, Compère P. Bacterial symbionts and mineral deposits in the branchial chamber of the hydrothermal vent shrimp *Rimicaris exoculata*: Relationship to moult cycle. Aquat Biol. 2008;1:225–38.
28. Corbari L, Cambon-Bonavita MA, Long GJ, Grandjean F, Zbinden M, Gaill F, et al. Iron oxide deposits associated with the ectosymbiotic bacteria in the hydrothermal vent shrimp *Rimicaris exoculata*. Biogeosciences. 2008;5:1295–310.
29. Reveillaud J, Anderson R, Reves-Sohn S, Cavanaugh C, Huber JA. Metagenomic investigation of vestimentiferan tubeworm endosymbionts from Mid-Cayman Rise reveals new insights into metabolism and diversity. Microbiome. 2018;6:19.
30. Charlou JL, Donval JP, Konn C, Ondréas H, Fouquet Y, Jean-Baptiste P, et al. High production and fluxes of H2 and CH4 and evidence of abiotic hydrocarbon synthesis by serpentinization in ultramafic-hosted hydrothermal systems on the Mid-Atlantic Ridge. Divers Hydrothermal Syst Slow Spreading Ocean Ridges. 2010;265–96.
31. Kato S, Kobayashi C, Kakegawa T, Yamagishi A. Microbial communities in iron-silica-rich microbial mats at deep-sea hydrothermal fields of the southern Mariana Trough. Environ Microbiol. 11: 2094–2111.
32. Suzuki MT, Taylor LT, DeLong EF. Quantitative analysis of small-subunit rRNA genes in mixed microbial populations via 5'-nuclease assays. Appl Environ Microbiol. 2000;66:4605–14.
33. Bushnell B, Rood J, Singer E. BBMerge – Accurate paired shotgun read merging via overlap. PLoS One. 2017;12:e0185056.
34. Köster J, Rahmann S. Snakemake—a scalable bioinformatics workflow engine. Bioinformatics. 2012;28:2520–2.
35. Eren AM, Esen ÖC, Quince C, Vineis JH, Morrison HG, Sogin ML, et al. Anvi'o: an advanced analysis and visualization platform for 'omics data. PeerJ. 2015;3:e1319.

36. Eren AM, Vineis JH, Morrison HG, Sogin ML. A filtering method to generate high quality short reads using Illumina paired-end technology. PLoS One. 2013;8:6–11.
37. Li D, Liu CM, Luo R, Sadakane K, Lam TW. MEGAHIT: An ultra-fast single-node solution for large and complex metagenomics assembly via succinct de Bruijn graph. Bioinformatics. 2015;31:1674–6.
38. Hyatt D, Chen GL, LoCascio PF, Land ML, Larimer FW, Hauser LJ. Prodigal: Prokaryotic gene recognition and translation initiation site identification. BMC Bioinformatics. 2010;11.
39. Aramaki T, Blanc-Mathieu R, Endo H, Ohkubo K, Kanehisa M, Goto S, et al. KofamKOALA: KEGG ortholog assignment based on profile HMM and adaptive score threshold. Bioinformatics. 2019;36:2251–2.
40. Garber AI, Nealson KH, Okamoto A, McAllister SM, Chan CS, Barco RA, et al. FeGenie: A comprehensive tool for the identification of iron genes and iron gene neighborhoods in genome and metagenome assemblies. Front Microbiol. 2020;11:1–23.
41. Langmead B, Salzberg SL. Fast gapped-read alignment with Bowtie 2. Nat Methods. 2012;9:357.
42. Chaumeil P-A, Mussig AJ, Hugenholtz P, Parks DH. GTDB-Tk: a toolkit to classify genomes with the Genome Taxonomy Database. Bioinformatics. 2019;36:1925–7.
43. Capella-Gutiérrez S, Silla-Martínez JM, Gabaldón T. trimAl: A tool for automated alignment trimming in large-scale phylogenetic analyses. Bioinformatics. 2009;25:1972–3.
44. Nguyen LT, Schmidt HA, Von Haeseler A, Minh BQ. IQ-TREE: A fast and effective stochastic algorithm for estimating maximum-likelihood phylogenies. Mol Biol Evol. 2015;32:268–74.
45. Whelan S, Goldman N. A general empirical model of protein evolution derived from multiple protein families using a maximum-likelihood approach. Mol Biol Evol. 2001;18:691–9.
46. Yoon S-H, Ha S, Lim J, Kwon S, Chun J. A large-scale evaluation of algorithms to calculate average nucleotide identity. Antonie Van Leeuwenhoek. 2017;110:1281–6.
47. Graham ED, Heidelberg JF, Tully BJ. Potential for primary productivity in a globally-distributed bacterial phototroph. ISME J. 2018;12:1861–6.
48. Lin X, Wakeham SG, Putnam IF, Astor YM, Scranton MI, Chistoserdov AY, et al. Comparison of vertical distributions of prokaryotic assemblages in the anoxic cariaco basin and black sea by use of fluorescence in situ hybridization. Appl Environ Microbiol. 2006;72:2679–90.
49. Campbell JH, O'Donoghue P, Campbell AG, Schwientek P, Sczyrba A, Woyke T, et al. UGA is an additional glycine codon in uncultured SR1 bacteria from the human microbiota. Proc Natl Acad Sci. 2013;110:5540–5.
50. Hug LA, Baker BJ, Anantharaman K, Brown CT, Probst AJ, Castelle CJ, et al. A new view of the tree of life. Nat Microbiol. 2016;1:1–6.
51. Herrmann M, Wegner CE, Taubert M, Geesink P, Lehmann K, Yan L, et al. Predominance of Cand. Patescibacteria in groundwater is caused by their preferential mobilization from soils and flourishing under oligotrophic conditions. Front Microbiol. 2019;10:1–15.

52. Sieber CMK, Paul BG, Castelle CJ, Hu P, Tringe SG, Valentine DL, et al. Unusual metabolism and hypervariation in the genome of a gracilibacterium (Bd1-5) from an oil-degrading community. MBio. 2019;10:1–14.
53. Yang Y, Sun J, Sun Y, Kwan YH, Wong WC, Zhang Y, et al. Genomic, transcriptomic, and proteomic insights into the symbiosis of deep-sea tubeworm holobionts. ISME J. 2020;14:135–50.
54. Costa TRD, Felisberto-Rodrigues C, Meir A, Prevost MS, Redzej A, Trokter M, et al. Secretion systems in Gram-negative bacteria: Structural and mechanistic insights. Nat Rev Microbiol. 2015;13:343–59.
55. Li Y, Liles MR, Halanych KM. Endosymbiont genomes yield clues of tubeworm success. ISME J. 2018;12:2785–95.
56. Maltz M, Graf J. The type II secretion system is essential for erythrocyte lysis and gut colonization by the leech digestive tract symbiont aeromonas veronii. Appl Environ Microbiol. 2011;77:597–603.
57. Moebius N, Üzüm Z, Dijksterhuis J, Lackner G, Hertweck C. Active invasion of bacteria into living fungal cells. Elife. 2014;3:e03007.
58. Pickering BS, Oresnik IJ. The twin arginine transport system appears to be essential for viability in Sinorhizobium meliloti. J Bacteriol. 2010;192:5173–80.
59. Beinart RA, Luo C, Konstantinidis KT, Stewart FJ, Girguis PR. The bacterial symbionts of closely related hydrothermal vent snails with distinct geochemical habitats show broad similarity in chemoautotrophic gene content. Front Microbiol. 2019;10:1–13.
60. Barco RA, Emerson D, Sylvan JB, Orcutt BN, Jacobson Meyers ME, Ramírez GA, et al. New insight into microbial iron oxidation as revealed by the proteomic profile of an obligate iron-oxidizing chemolithoautotroph. Appl Environ Microbiol. 2015;81:5927–37.
61. He S, Barco RA, Emerson D, Roden EE. Comparative genomic analysis of neutrophilic iron(II) oxidizer genomes for candidate genes in extracellular electron transfer. Front Microbiol. 2017;8:1–17.
62. Le Bloa S, Durand L, Cueff-Gauchard V, Le Bars J, Taupin L, Marteau C, et al. Highlighting of quorum sensing lux genes and their expression in the hydrothermal vent shrimp *Rimicaris exoculata* ectosymbiontic community. Possible use as biogeographic markers. PLoS One. 2017;12:1–19.
63. Waters RC, O'Toole PW, Ryan KA. The FliK protein and flagellar hook-length control. Protein Sci. 2007;16:769–80.
64. Markert S, Arndt C, Felbeck H, Becher D, Sievert SM, Hügler M, et al. Physiological proteomics of the uncultured endosymbiont of *Riftia pachyptila*. Science. 2007;315:247–50.
65. Gulmann LK, Beaulieu SE, Shank TM, Ding K, Seyfried WE, Sievert SM. Bacterial diversity and successional patterns during biofilm formation on freshly exposed basalt surfaces at diffuse-flow deep-sea vents. Front Microbiol. 2015;6:1–16.
66. Stokke R, Dahle H, Roalkvam I, Wissuwa J, Daae FL, Tooming-Klunderud A, et al. Functional interactions among filamentous Epsilonproteobacteria and Bacteroidetes in a deep-sea hydrothermal vent biofilm. Environ Microbiol. 2015;17:4063–77.

67. Fouquet Y, Cambon P, Etoubleau J, Charlou JL, Ondréas H, Barriga FJAS, et al. Geodiversity of hydrothermal processes along the Mid-Atlantic Ridge and ultramafic-hosted mineralization: A new type of oceanic Cu-Zn-Co-Au volcanogenic massive sulfide deposit. Geophys Monogr Ser. 2013;188:321–67.
68. McKay LJ, Dlakić M, Fields MW, Delmont TO, Eren AM, Jay ZJ, et al. Co-occurring genomic capacity for anaerobic methane and dissimilatory sulfur metabolisms discovered in the Korarchaeota. Nat Microbiol. 2019;4:614–22.
69. Reveillaud J, Bordenstein SR, Cruaud C, Shaiber A, Esen ÖC, Weill M, et al. The *Wolbachia* mobilome in *Culex pipiens* includes a putative plasmid. Nat Commun. 2019;10:1051.
70. Aschtgen MS, Brennan CA, Nikolakakis K, Cohen S, McFall-Ngai M, Ruby EG. Insights into flagellar function and mechanism from the squid–vibrio symbiosis. npj Biofilms Microbiomes.2019;5.
71. Nelson DC, Hagen KD, Edwards DB. The gill symbiont of the hydrothermal vent mussel *Bathymodiolus thermophilus* is a psychrophilic, chemoautotrophic, sulfur bacterium. Mar Biol. 1995;121:487–95.
72. Chun J, Oren A, Ventosa A, Christensen H, Arahal DR, da Costa MS, et al. Proposed minimal standards for the use of genome data for the taxonomy of prokaryotes. Int J Syst Evol Microbiol. 2018;68:461–6.
73. Holmes AJ, Kelly DP, Baker SC, Thompson AS, Marco P, De, Kenna EM, et al. *Methylosulfonomonas methylovora* gen. nov., sp. nov., and *Marinosulfonomonas methylotropha* gen. nov., sp. nov.: novel methylotrophs able to grow on methanesulfonic acid. Arch Microbiol. 1997;167:46–53.
74. Ansorge R, Romano S, Sayavedra L, Porras MÁG, Kupczok A, Tegetmeyer HE, et al. Functional diversity enables multiple symbiont strains to coexist in deep-sea mussels. Nat Microbiol. 2019.
75. Ikuta T, Takaki Y, Nagai Y, Shimamura S, Tsuda M, Kawagucci S, et al. Heterogeneous composition of key metabolic gene clusters in a vent mussel symbiont population. ISME J. 2016;10:990–1001.
76. Grzymski JJ, Murray AE, Campbell BJ, Kaplarevic M, Gao GR, Lee C, et al. Metagenome analysis of an extreme microbial symbiosis reveals eurythermal adaptation and metabolic flexibility. Proc Natl Acad Sci U S A. 2008;105:17516–21.
77. Alcaide M, Tchigvintsev A, Martínez-Martínez M, Popovic A, Reva ON, Lafraya Á, et al. Identification and characterization of carboxyl esterases of gill chamber-associated microbiota in the deep-sea shrimp Rimicaris exoculata by using functional metagenomics. Appl Environ Microbiol. 2015;81:2125–36.
78. Teixeira S, Cambon-Bonavita M-A, Serrão EA, Desbruyéres D, Arnaud-Haond S. Recent population expansion and connectivity in the hydrothermal shrimp *Rimicaris exoculata* along the Mid-Atlantic Ridge. J Biogeogr. 2011;38:564–74.
79. Declarations.

Figures

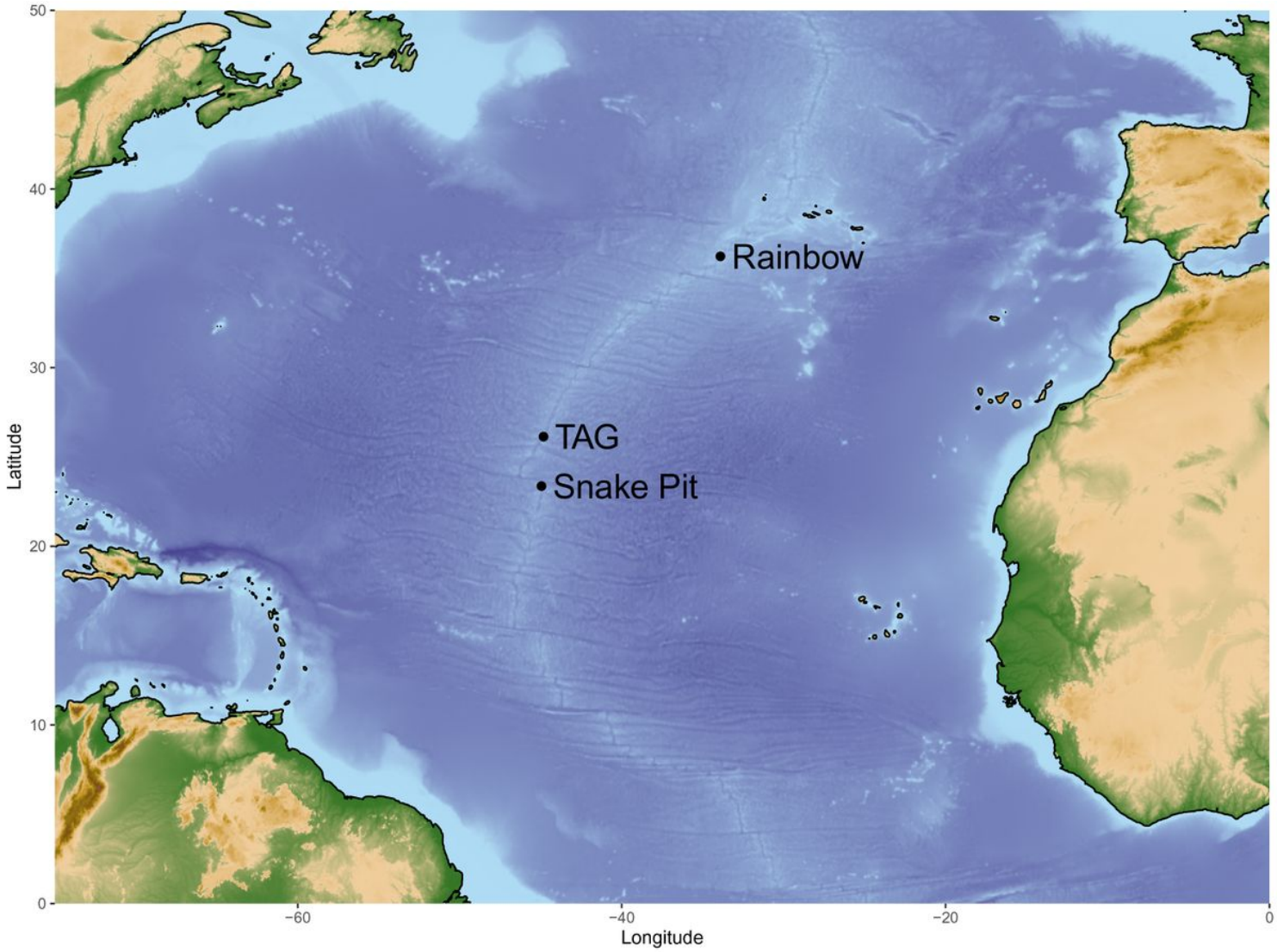

Figure 1

Geographic locations of Mid-Atlantic Ridge hydrothermal vent sites Rainbow, TAG and Snake Pit where Rimicaris specimen were sampled.

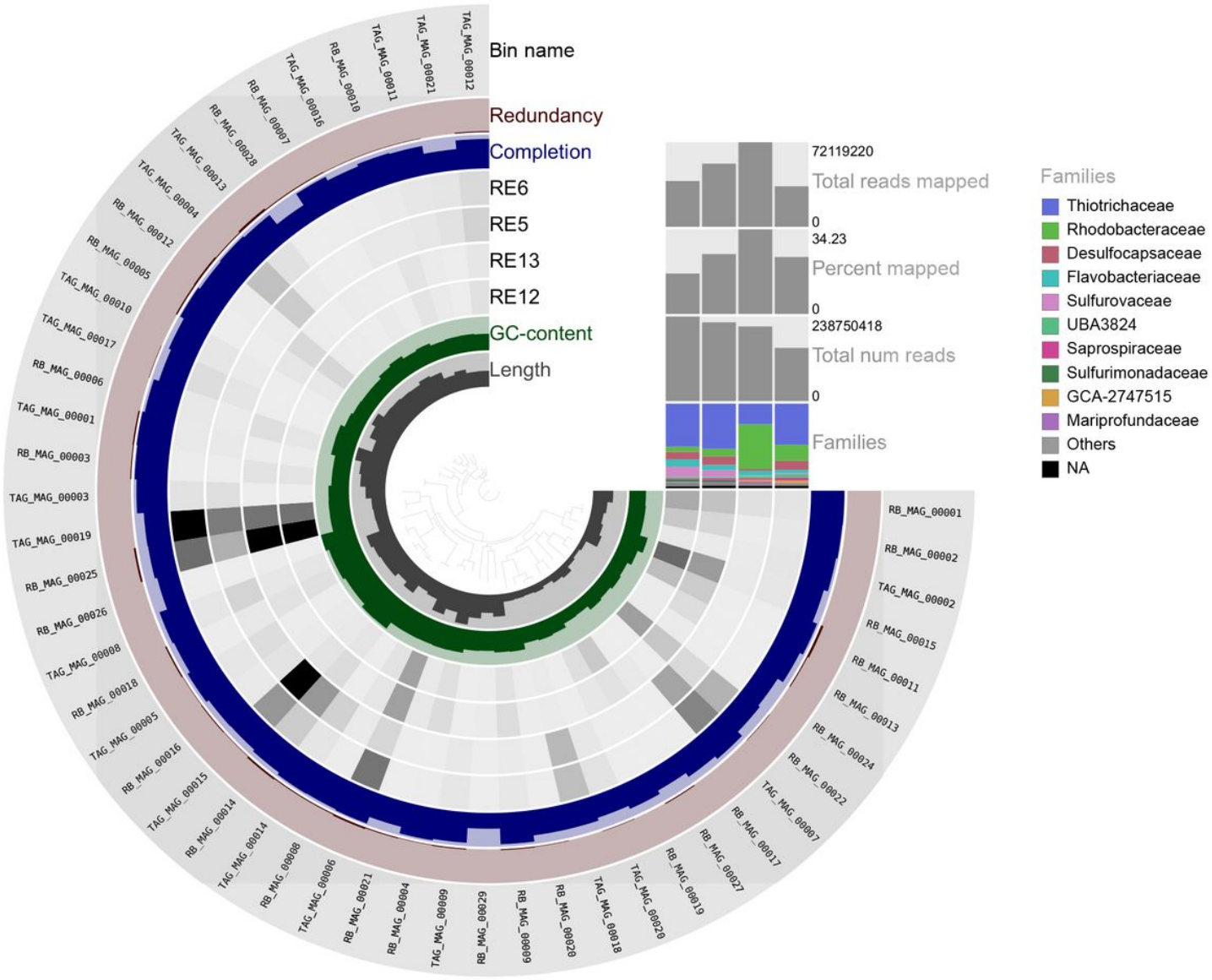

Figure 2

Static image from the anvi'o interactive display for the Rimicaris datasets with the 49 genome bins retained for this study. From inner to outer layers: phylogenomic tree based on concatenated marker proteins according to the GTDB-Tk genome phylogeny as described below (see Figure 4), length layer (shows the actual length of a given split), auxiliary layer with information about contigs stored in the contig database (GC-content), 4 view layers with information about MAGs across samples stored in the profile database (mean coverage), completion, redundancy and bacterial genome bin layers. The horizontal layers show genome bins taxonomy based on GTDB_TK for the ten most abundant families, total number of reads for each sample, total number of reads mapping and corresponding mapping percent of reads. Relative abundances of families are noted as the percent of reads recruited to the bins for each sample.

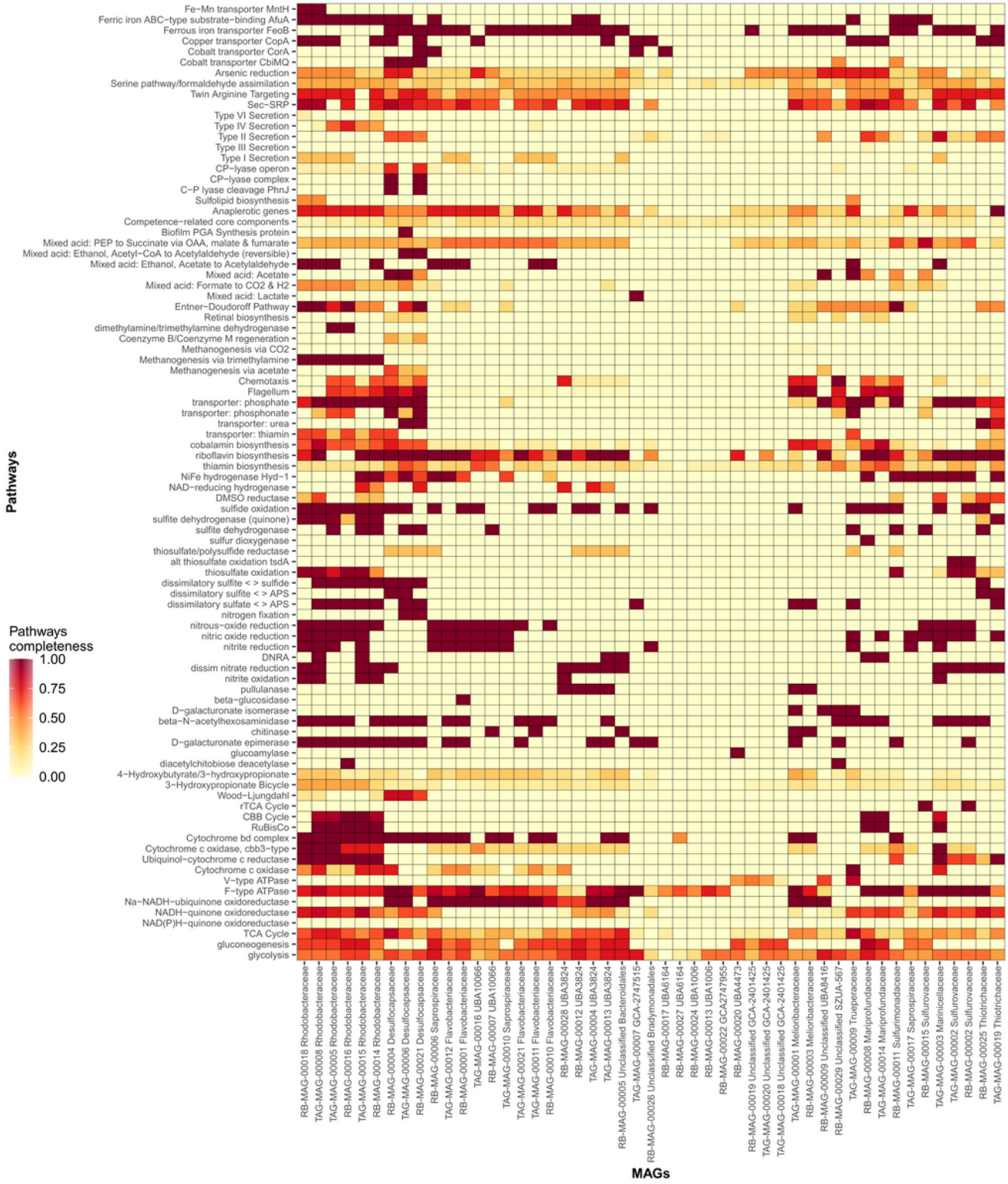

Figure 3

Decodder output; MAGs and predicted metabolic function.

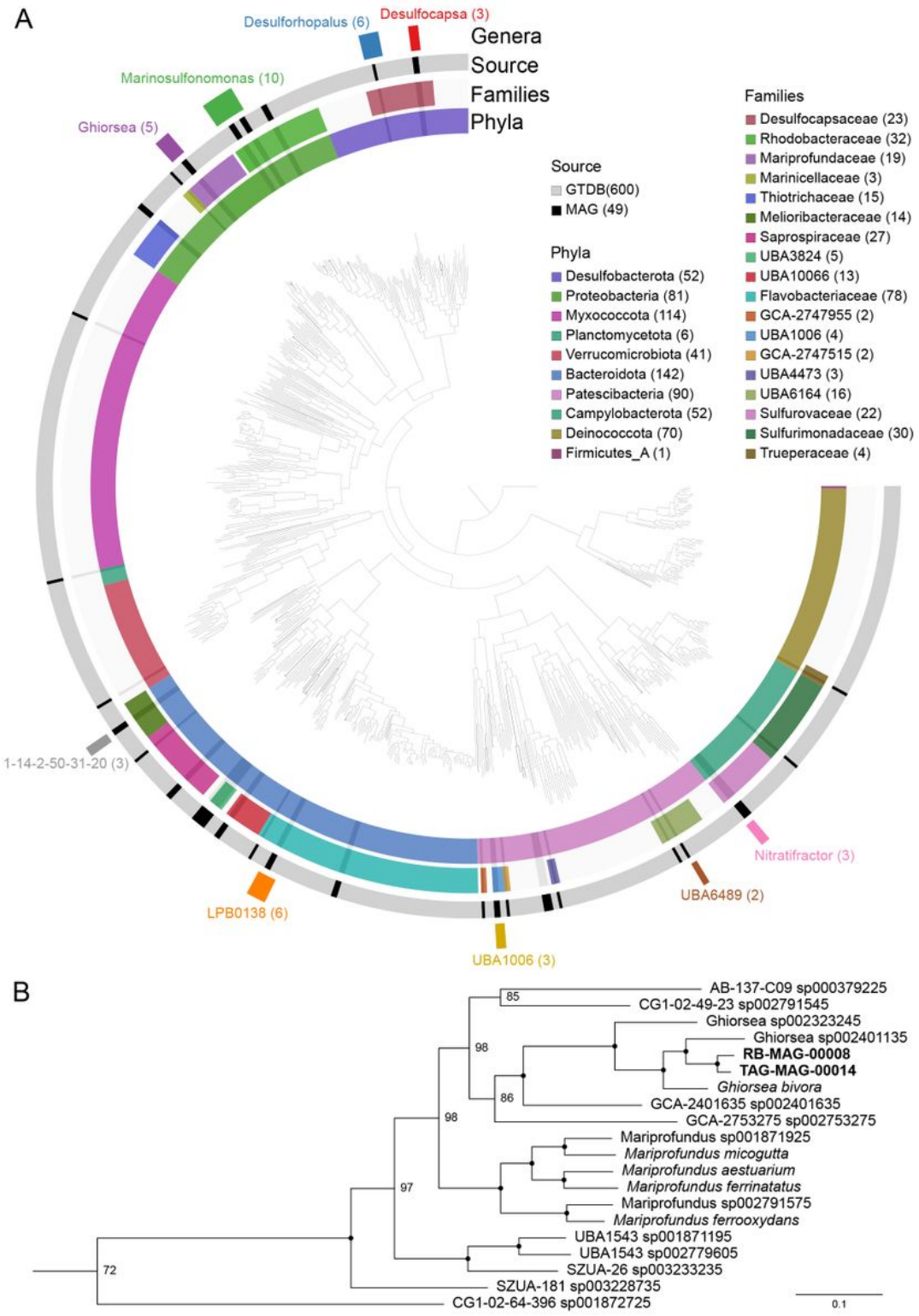

Figure 4

A.Maximum-likelihood tree based on concatenated marker proteins according to the GTDB-Tk genome phylogeny visualized using anvi'o. Tree includes 600 genomes from GTDB and 49 MAGs covering mostly unknown genera, highlighting the importance of lineages lacking representatives. A single Firmicutes was used to root the tree. The bars in the innermost circular layer show the phylum affiliation of each genome. The second layer represents the family affiliation. The third layer marks genomes as either MAGs from

our study (49, black) or genomes from GTDB (grey). The outermost layer shows the genera affiliation (10) and the lack thereof (19) of our MAGS. Only the families and genera observed in the MAGs are shown. B. Zoom inset of the Zetaproteobacteria phylogenetic relationships visualized using FigTree. Nodes represented by a dot indicate a bootstrap value of 100; lower values are given.

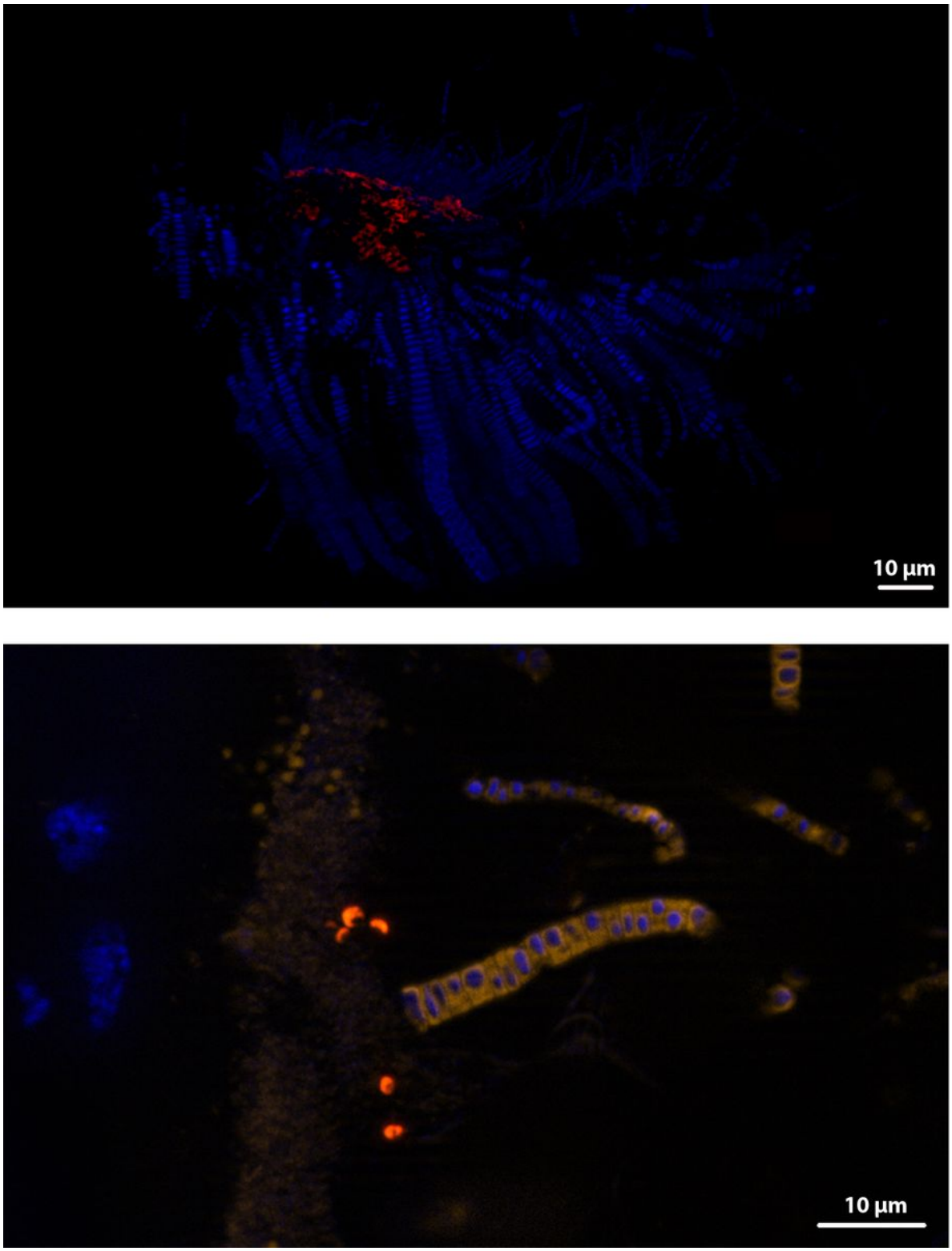

Figure 5

FISH observation of a Rainbow R. exoculata branchiostegite with epibionts. All cells are labelled with DAPI (blue). Zetaproteobacteria are hybridized with the Zeta123 probe (red) [23]. Campylobacteria are hybridized with the EPSI 549 probe (orange) [48].

Supplementary Files

This is a list of supplementary files associated with this preprint. Click to download.

- SupplementaryMaterial1stJune2020.docx